Chloride transport in partially saturated mortar made of blended cement

Zhang, Yong; Ye, Guang

Publication date
2015

Document Version
Accepted author manuscript

Published in
Proceedings of the 14th International Congress on the Chemistry of Cement

Chloride transport in partially saturated mortar made of blended cement

Yong Zhang[1]*, Guang Ye[1]

1. Microlab, Civil Engineering and Geoscience, Delft University of Technology, 2628 CN Delft, The Netherlands

Abstract

Due to environmental (low CO_2 emission) and economic benefit, supplementary cementitious materials (SCMs) have been widely used in reinforced concrete structures. However, the question from engineering practice is to which extend these blended mixtures do meet the future durability criteria. Chloride ingression is nowadays considered as the main concern for reinforcement corrosion. Due to self-desiccation or drying process, cement-based materials are no longer saturated, which would greatly influence the chloride transport properties.

This paper explores the effect of water saturation level on chloride diffusivity in cement-based materials by resistivity measurements. Experiments were performed on mortars made of different blended materials, i.e. fly ash, blast furnace slag and limestone powder. Mortar materials have been curing for 200 days conditioning in humid room at 20±1°C, followed by oven drying at 50°C until the samples reach targeted water saturation levels. The results showed that chloride diffusivity is highly dependent on the water saturation level and water-vapour desorption isotherm of the mortar material. The dependency varies with cement type, and is significantly related to pore size distribution characteristics. In addition, the effect of water content on chloride diffusivity is more evident in blended cement mortars than reference ordinary Portland cement mortar. For the materials studied in this research, the capillary pores with diameter range of 7.1-73 nm plays dominated role in chloride diffusion under non-saturated state.

Keywords: *relative diffusivity; saturation degree; chloride; supplementary cementitious materials*

* **Corresponding author: y.zhang-1@tudelft.nl, Tel +31-681776151**

1. Introduction

Due to the environmental and economic benefit, nowadays supplementary cementitious materials (SCMs), such as ground granulated blast-furnace slag (BFS), fly ash (FA), limestone powder (LP), have been widely incorporated into binary, ternary and quaternary cement concrete mixes. Nevertheless, the durability of these blended materials remains uncertain yet. Chloride diffusivity is usually considered as main indicator to evaluate the durability of reinforced concrete serving in marine environment. Chloride ions can penetrate into cement-based materials through connected aqueous solution in the porous network. Whenever the critical amount of chloride ions reaches the surface of reinforced steel, along with enough oxygen and moisture, steel corrosion may take place resulting in cracking and spalling of the cover concrete. The time from casting of concrete to corrosion initiation of reinforced steel is usually defined as service life of reinforced concrete structures.

The current standard, e.g. Duracrete, relies on measurement of chloride transport in saturated concrete, and the service life prediction is designated on diffusion model which is deduced by Fick's second law. However, concrete is seldom saturated due to its long term self-desiccation or drying process. It was reported that even under water stored concrete remains unsaturated after 220 days' curing age (Powers *et al.* 1947). A series of experiments have also proved that the relative humidity of interior concrete could be as low as 75% even if the concrete is curing under water for long time (Nilsson 1980; Chatterji 1995; Bertil 2001). Actually, concrete is very difficult to re-saturate once the unsaturated state has achieved (Glasser *et al.* 2001). Chatterji (2004) illustrated this phenomenon on the basis of hydrodynamics of water flow through concrete, and pointed out that it often takes years to re-saturate after contact with water. It is known that the moisture diffusivity of cement-based materials is usually no more than 1.0×10^{-12} m^2/s, take sample with 10 mm in thickness as example, the diffusion time required for saturation is around 3 years (Galle *et al*. 2000). In most cases, steel corrosion occurs in unsaturated concrete. Chloride transport approaches, based on Fick's second law alone, not involving unsaturated condition, have no real practical interest.

Chloride penetration is a humid process, and occurs only if water is present. In saturated condition, all the pores in concrete are fulfilled with water solution. Diffusion through the water-filled porous network is believed to be the main mechanism for chloride penetration. Under non-saturated condition, water phase favours to fill the smaller pores, and the moisture profile inside porous network would be distributed in different manner from that in saturated condition. As a result, the chloride penetration becomes much more complex. Nevertheless, the chloride transport properties under non-saturated condition were seldom noticed in previous lab-experiments and analysis, and very little progress has been made in this research field, possibly because of the difficulties in sample preparation and chloride penetration test in unsaturated state.

This paper attempt to investigate the chloride diffusivity in partially saturated mortar made of blended cement. The pore structures as well as water-vapour desorption isotherms were measured. The chloride diffusivity was assessed by resistivity measurements. The pore structure was evaluated by mercury intrusion porosimetry (MIP). The results showed that chloride diffusivity is highly dependent on the water saturation level and water-vapour desorption isotherm of the mortar material. Compared to reference ordinary Portland cement mortar, the effect of water content on chloride diffusivity is more evident in blended cement mortars, which is determined by pore size distribution of the materials.

2. Experiments

2.1. Raw Materials

In the experimental program, both cement paste and mortar was studied. The binder material is a mixture of ordinary Portland cement (OPC) blended with fly ash (FA), blast furnace slag (BSF) or limestone powder (LP). The mixture proportions for cement pastes are listed in table 1. Water to binder ratio (W/B) is 0.5 and the curing age is 200 days for all mixtures. Mercury intrusion porosimetry (MIP) is performed to determine the pore structure of cement pastes. The sample preparation for MIP can be found elsewhere in (Ye 2003).

Mortar samples were cast for desorption isotherm test and resistivity measurement. Each mortar was made with the same content of siliceous sand, but varies with binders. The particle size of siliceous sand ranges from 0.125 mm to 2 mm. The binder to sand ratio is 1:3 by weight. Cylindrical mortars 800 mm in height and 100 mm in diameter were cast in the lab, which were demoulded after one day curing. The mortars were then moved to humid curing room at 20±1°C. After curing 200 days, both the top and bottom surface of the mortar samples with the thickness of 15 mm were cut off with a diamond blade saw, the middle part of the samples will follow the sample preconditioning procedure which is described in subsequent section 2.2.

Tab. 1 Mixture proportions (weight percentage) used for the binders

Binder	OPC	FA	BFS	LP	W/B
P	100%	-	-	-	0.5
PF	70%	30%	-	-	0.5
PB	30%	-	70%	-	0.5
PBL	25%	-	70%	5%	0.5

2.2 Sample preconditioning

A well-controlled partial saturation state must be obtained before resistivity measurements. Water saturation degree (SD) is a measure of moisture content in the porous network. It is defined as the volume fraction of voids filled with water over the total volume of voids, which can be expressed in equation (1):

$$SD = \frac{m_h - m_d}{m_s - m_d} \quad (1)$$

where m_h is the mass of specimen at particular saturation state (g), m_s is the mass of specimen at saturated condition (g), m_d is the mass of dried specimen (g).

In this research, 50-mm thick discs of mortar samples were preconditioned to different SD values. Both the lateral and bottom sides were sealed with electric isolating tape to avoid any multi-side directional moisture transfers. Then the mortar samples were placed in a ventilated oven and heated at 5°C per hour up to 50°C. The oven was subsequently pumped until vacuum at 50 Pa to prevent carbonation. The mass loss with time was recorded. This involves recording decrement of mass change at relatively frequent intervals during the first 6 hours, and subsequently takes one measurement per day afterwards. The measurement precision of the balance is 0.001 g.

The sample mass corresponding to a particular SD, m_h, is calculated according to equation (2):

$$m_h = m_s \cdot \frac{1+SD \cdot A}{1+A} \quad (2)$$

where, A is the water absorption coefficient (%). The parameters m_s, m_d and A are obtained by following recommendation ASTM C642-13 (2013).

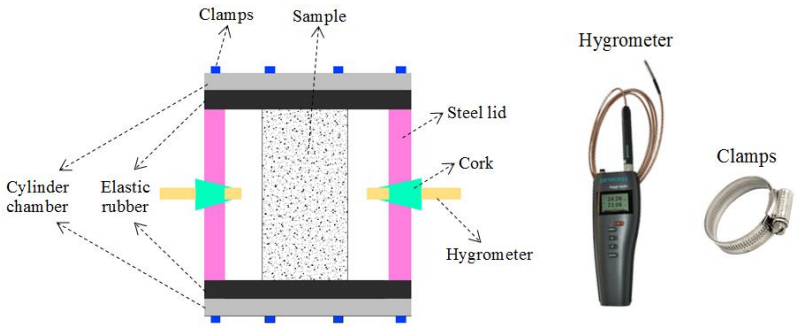

Figure 1 Set-up for monitoring the moisture homogeneity of mortar samples

As soon as m_h reaches its targeted value, there is still a moisture gradient from the bottom side to topside of the sample. In order to obtain homogeneous moisture distribution, a moisture redistribution step becomes a necessity. In this research, a simple set-up was developed to monitor and validate the moisture homogeneity inside samples, which was displayed in figure 1. Before moisture redistribution step, the electric isolating tape on the bottom surface of mortar sample was removed, with the lateral side still sealing. Next the mortar sample was placed in a cylinder tube and sealed thereafter,

maintaining constant temperature at 50°C. The time-related RH of both top and bottom surface of the sample were monitoring with the same type of hygrometer. As expected, the RH is increasing on top surface while decreasing on the bottom surface. Once the RH values on both surfaces are approaching identical (difference less than 1%), the moisture inside mortar sample can be assumed to be homogeneous. Then, the mortar sample was cooling down slowly with 5°C per hour to room temperature to avoid any initiation of crack. Finally, each mortar sample was moved out from the tube and stabilized in a plastic bag at its corresponding saturation state before any kind of measurement.

The protocol for sample preconditioning at each particular SD can be summarized briefly in Fig. 2.

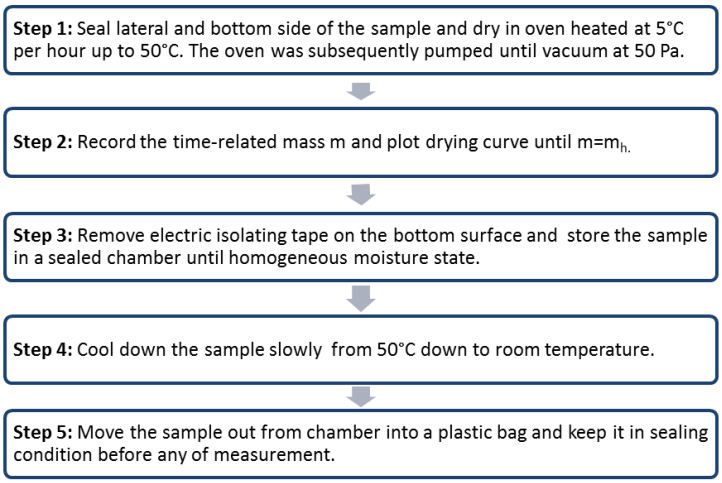

Figure 2 Sample preconditioning for mortar samples until targeted saturation degree

2.3 Mercury intrusion porosimetry (MIP)

Mercury intrusion porosimetry (MIP) is a technique commonly used to evaluate the pore structure characteristics of cementitious materials (Ye 2003). However, the notably ink-bottle problem makes the results inappropriate to describe the real pore size distribution (Diamond 2000). It has been reported that the 2nd cycle of MIP measurement has little "ink bottle" effect, and the pore size distribution obtained by 2nd mercury intrusion agrees very well with that derived from nitrogen sorption [Kaufmann 2009]. In addition, the ink-bottle pores not counted in the 2nd cycle mercury intrusion are relatively large in size (diameter > 100 nm) [Kaufmann 2009]. In this study, the pore diameter formed by meniscus curvature in unsaturated state is the research focus, which is usually smaller than 0.1 um. Therefore, the 2nd cycle of MIP can be an effective technique in this research.

The measurements were performed on paste materials with devise of Micrometrics Pore Sizer 9320. Each measurement was conducted by five stages: (1) a manual low pressure intrusion run from 0 to 0.17 MPa, (2) an automated high pressure intrusion run from 0.17 to 210 MPa, (3) an automated high pressure extrusion run from 210 MPa down to 0.03 MPa, (4) a 2nd high pressure intrusion run from 0.03 up to 210 MPa, (5) a 2nd automated high pressure extrusion run from 210 MPa down to 0.03 MPa. The equilibrium time for each applied pressure level was controlled at 30s. The test procedure can be found elsewhere in (Ye 2003). The result from the fourth stage of each measurement is used to identify the pore size distribution of paste sample. Three parallel measurements were performed.

To quantify the diameter of pore sizes, Washburn equation applies,

$$D = -\frac{4\gamma_{Hg}\cos\theta}{P} \quad (3)$$

where, P is the intrusion pressure of mercury. D is the equivalent pore diameter. γ_{Hg} is the surface tension of mercury and assumed as 0.48 N/m. The contact angle θ is 138°C.

2.4 Desorption isotherm

In order to study the moisture profile under different saturation levels, water-vapour desorption isotherm was measured on all the mortar samples. The lateral surfaces of each mortar sample were

sealed with electric isolating tape. The mortar samples with targeted SD levels were carried out with RH measurements, the correlation of SD and RH was established.

The RH in cementitious system is mainly controlled by the meniscus curvature formed in the pores. In principle, Kelvin-Laplace equation allows for calculation of menisci with diameter as low as 8 nm, with ±6% discrepancy for diameter in the range 8-40 nm (Leonard 1981). Kelvin-Laplace is shown in equation (4)

$$\ln(RH) = -\frac{2\gamma V_m \cos\theta}{rRT} \tag{4}$$

In this study, the thickness t of absorbed water film is taken into account (shown in Figure 3). Then, the Kelvin-Cohan equation should be applied (Neimark *et al*. 2003).

$$\ln(RH) = -\frac{2\gamma V_m \cos\theta}{(r+t)RT} \tag{5}$$

where, γ is surface tension of water (0.072 N/m in pure water), M is molar weight of water (0.01802 kg/mol), θ is contact angle between water and solids (herein assuming it is zero), V_m is the molar volume of water fluid, r is radius of the meniscus, R is ideal gas constant (8.314 J/mol·K) and T is absolute temperature, t is thickness of absorbed water film and expressed in nm. According to Badmann *et al.* (1981), t is a function of interior RH in the porous system and usually within 0.2-2 nm for cement-based materials:

$$t = 0.385 - 0.189 \cdot \ln(-\ln(RH)) \tag{6}$$

Based on Kelvin-Cohan equation, the maximum diameter for pores filled with water corresponding to a particular RH level can be obtained.

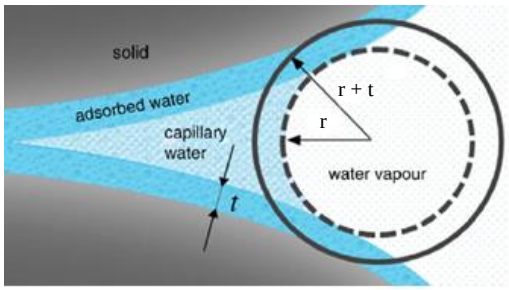

Figure 3 Schematic illustration of meniscus curvature and adsorbed water films in capillary pores [Chen 2013]

2.5 Electrochemical impedance spectroscopy (EIS)

In order to measure chloride diffusion coefficient in cement-based materials, chloride source was usually applied from the outer surface into the material. However, in unsaturated state, it is very difficult to perform chloride penetration without changing the interior water content of the material. Electrochemical Impedance Spectroscopy (EIS) has been widely used to investigate electrochemical system, which allows assessing the transport properties of cementitious materials (Olsson 2013). The bulk conductivity [σ] is theoretically correlated to the chloride diffusion coefficient [D]. According to Nernst-Einstein equation

$$\frac{\sigma}{\sigma_0} = \frac{D}{D_0} \tag{7}$$

where σ_0 (S/m) and D_0 (m^2/s) are the conductivity and diffusion coefficient of chloride ion through pore solution of cement-based materials.

In this research, the chloride diffusivity is assessed by resistivity measurement. A portable resistance meter, type ESCORT LCR using alternating current (AC) at 120 Hz was used for resistivity test in this study. For the specimens with each SD, the resistivity was measured with one stainless electrode covering each side of the specimen. Humid sponge was employed in between surface specimen and each electrode to ensure the whole surface of specimen under current flow. The measurements were performed at constant room temperature at 20°C. During the test, the measured resistivity was found to decrease with the time elapse. This is ascribed to the moisture loss of sponge

absorbed by the specimen. In this respect, only the first measurement was employed for the final analysis.

3. Results and discussions

3.1 Pore size distribution

The result of cumulative intrusion volume from 2nd cycle of MIP was applied to identify the pore size distribution of four paste materials. The pore size distribution curves are displayed in Fig. 4. It is found that, the most porosities are contributed by the pores with diameter less than 0.1 um. There is one main peak for each curve. With the addition of blended materials, the pore sizes toward to a finer distribution, and the peak corresponds to smaller pore sizes than the reference system P. The smallest peak was observed in slag-blended system PB. Interestingly to note that the pore size distribution of mixtures PF and PBL are quite approaching to each other. The influence of pore size distribution on water-vapor desorption isotherm as well as on chloride diffusivity will be discussed in the following sections.

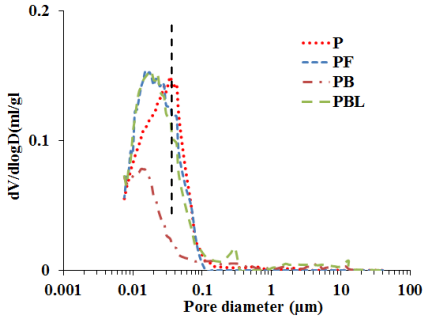

Figure 4 Pore size distributions of paste materials identified by 2nd cycle of MIP

3.2 Water-vapor desorption isotherm

In order to understand the moisture profile at each particular saturation state, water-vapour desorption isotherms were investigated. The results for all the mortar mixtures were plotted in figure 5, which present the relative humidity (RH) at each targeted SD level. As indicated, the four mixtures follow similar evolution, and each curve can be divided into two stages for the tested SD range. However, strong differences lie in the results at high SD levels. When the SD decreases from saturated state, the RH for reference mortar P starts with a slight decrease but was followed by a relatively steeper linear drop. On the contrary, for blended mortars, the curves tend to start with a sharp decrease and thereafter a linear slowly decrease is followed. In addition, blended mortars present much higher saturation level corresponding to very low interior RH than reference mortar P. For example, with SD of 80%, the interior RH is 75% in slag-blended mortar (PB), while this value is as high as 95% in reference mortar P. According to Kelvin-Laplace equation, the higher interior RH corresponds to a larger meniscus radius. At the same water saturation level (e.g. 80%), the meniscus radius is lower in blended cement mortars. This is in agreement with the results of finer pore size distribution of paste matrix, which is shown in Figure 4. It should be also noted that, the curves of mixtures PF and PBL are very closed compared to the other two curves. This might be highly related to the similar pore size distribution characteristics of corresponding paste matrix, as shown in Figure 4. In fact, when the RH is decreasing from 95% down to 45%, the diameter of meniscus curvature formed in the porous network declines from 42 nm to 3 nm, which highlights the decisive role of small capillary pore size on the moisture distribution in unsaturated state.

The fall of interior RH in desorption isotherm can be associated with a percolating pore network that draining with decrease of SD. Water desorption occurs by vapour diffusion in the porous network, the draining of a pore is possible only when this pore is connected to the draining network. A reduction in SD leads to a reduction in RH. In contrast, the air void space increases, which may decrease the possibility of connections of water solution in the percolating pore network and thus

influence the ionic diffusion. For this reason, water-vapour desorption isotherm should be highly linked to chloride penetration in unsaturated state, which depends on the pores and their size range of percolating network. This point will be further discussed in following section.

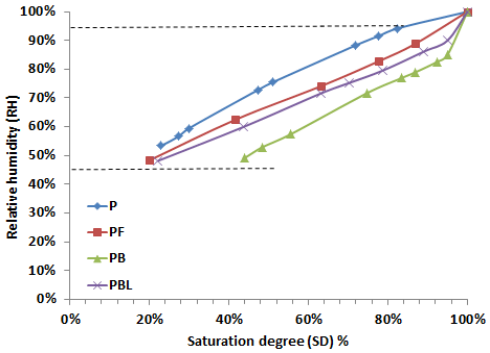

Figure 5 Relative humidity is a function of saturation degree in mortar materials

3.3 Relative chloride diffusivity vs. saturation degree

The resistivity measurements were performed on all the mortar specimens. It should be noted that some specimens with very low SD failed to be measured with the resistance meter, because the resistance is too high to be tested. In these cases, the pore solution in the material is assumed to be discontinuous. In other words, the depercolation for chloride diffusion has attained. The corresponding water saturation related to the depercolation for chloride diffusion is noted in this paper as "critical saturation level". Based on Nernst-Einstein equation, the resistivity results were expressed in terms of diffusivity coefficient. The relative diffusivity is defined as the ratio of chloride diffusivity at given SD over that under saturated condition.

The relative chloride diffusivity is analyzed against water saturation degree. The results are summarized in figure 6. Apparently, relative chloride diffusivity is highly dependent on SD regardless of binder type. It starts with slightly decrease when the water starts to loss from saturated state, but then falls off rapid when SD is in between 60%-95%, followed by a slow drop and finally approaches to zero at SD value near 40%. With the decrease of SD, the chloride diffusion would be impaired by the decrease of the number of transport channels, which are interconnected and filled with water solution. Also, as the decrease of the thickness of adsorbed water layers, chloride diffusion can be interfered by the precipitation of chemical compound (e.g. $Ca(OH)_2$) as well as by the strong rise of the interaction forces between cement paste and ions (Saetta 1993). Particularly at the very low saturation level, the chloride diffusivity is negligible. Possibly because there is no longer continuous penetration path through the porous network, thus preventing significantly chloride diffusion.

It should be noted that, compared with reference mortar P, the relative chloride diffusivities in blended mortars are much more sensitive to the changes of water saturation level. At given SD, the highest relative chloride diffusivity is observed in reference mortar P, followed by mortar PF, PBL and PB. If look it in detail, at SD of 80%, the chloride diffusivities in blended mortars are 10% (PB), 30% (PBL) and 35% (PF) respectively over that under saturated condition, while this value is 60% in reference mortar P.

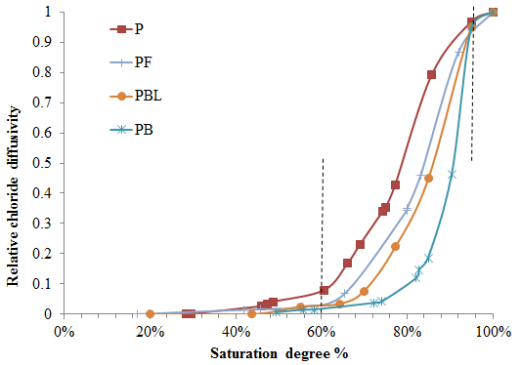

Figure 6 Relative chloride diffusivity depends on saturation degree

According to Kaufmann (2009), the ink-bottle pores from the first mercury intrusion measurement are relatively large in size (diameter > 0.1 um), and the second cycle of mercury intrusion measurement showed very little ink-bottle effect. In this regards, it can be assumed that the capillary pores of small size range (e.g. diameter < 0.1 um) are connected through the bridge of large capillary pores (e.g. diameter > 0.1 um). The small capillary pores act as throat neck in the porous channels, which govern the interior RH level as well as the chloride diffusion process. At given SD/RH level, the maximum diameter of throat pores, which are fulfilled with water solution, can be determined by Kelvin-Cohen equation. This maximum diamater of throat pore, corresponding to a particular SD/RH value, is defined in this paper as “percolating diameter”. The pores at each percolating diameter are denoted as “percolating pores”. In unsaturated state, it is the throat pores with size range less than percolating diameter that provide the main paths for ionic diffusion. The percolating diameter is decreased with the decrease of SD/RH level. Accordingly, the pore family in view of chloride diffusivity can be categorized into three portions based on their size distributions: (1) pores with size range larger than the biggest percolating pore, herein noted as macro pores; (2) percolating pores; (3) pores with size range smaller than smallest percolating pore, herein noted as micro pores. The schematic details are illustrated in figure 7.

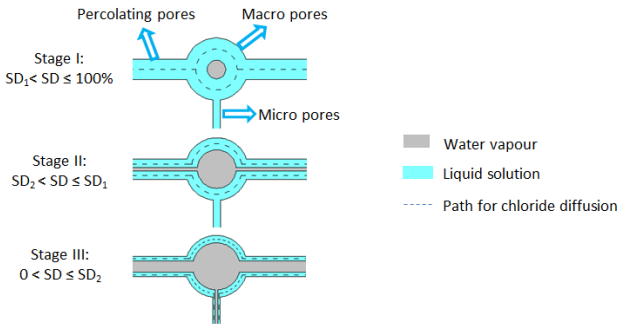

Figure 7 Schematic porous channels and ionic diffusion with the decrease of water saturation degree

The relative chloride diffusivity in relation to SD can be consequently divided into three stages:

I. All the percolating pores are saturated. When SD starts to decrease from saturated state (SD < 100%), the macro pores firstly loss water, the main routes for chloride diffusion are remain saturated with pore solution. The chloride diffusivity is not severely influenced and quite closed to that in saturated condition.
II. With the decrease of SD level ($SD<SD_1$), the percolating pores are partially saturated. In this stage, the percolating pores start to loss water, and are gradually filled with water vapour. Subsequently, chloride diffusion is significantly influenced, and a sharp decrease in relative diffusivity was observed. The scope of SD level in this stage is defined as sensitive SD with respect to chloride diffusivity.
III. Once the SD is lower than a critical level SD_2, all of percolating pores are unsaturated and absorbed with solution layers, which are composed of water molecules and chemical

compounds (e.g. $Ca(OH)_2$). In this stage, water loss commences in micro pores. The diffusion process is quite slow but decreases less apparently until depercolation attained.

The diameter range of percolating pores can be obtained from stage II. As indicated in figure 6, the sensitive SD ($SD_2<SD<SD_1$) for reference mortar P is in the range of 60%-95%, corresponding to interior RH range 80%-97% (from figure 5). On the basis of Kelvin-Cohen equation, the associated percolating diameter can be figured out that is ranging from 10.8-73.0 nm. From pore size distribution curve (figure 4), the volume percentage of percolating pores (diameter 10.8-73.0 nm) over the total pore volume is 46.4% for reference system P. Accordingly, the results for blended systems can be derived as well. The overall results are summarized in Table 2. As it is presented, the volume percentage of percolating pores is much less in blended systems than reference system P. As a result, the water continuity of percolating pores in blended systems would be more sensitive to the loss of water and decreases much faster with the decrease of SD. Consequently, the effect of SD on relative diffusivity is more evident in blended mortar samples.

Tab. 2 Calculation of percolating pores with related to chloride diffusivity in unsaturated state

Mixtures	Sensitive SD range ($SD_2<SD<SD_1$)	Corresponding RH range	corresponding percolating diameter	Volume percentage of percolating pores
P	60-95%	80-97%	10.8-73.0 nm	46.4%
PF	65-95%	75-95%	8.6-43.4 nm	33.8%
PBL	70-95%	75-95%	7.1-43.4 nm	25.2%
PB	80-95%	75-85%	8.6-14.5 nm	13.7%

4. Conclusions

This paper studied the chloride diffusivity in unsaturated state of various cement-based materials by resistivity measurements. The water-vapour desorption isotherm was obtained based on the measurement of relative humidity against each water saturation level. The pore structure was analyzed and discussed with relation to moisture profile as well as to chloride diffusivity under non-saturated condition. It was found that chloride diffusivity of cement-based materials is highly dependent on the water content and water desorption isotherm, the dependency is significantly related to pore size distribution of the material. Compared with OPC system, the effect of SD on chloride diffusivity in blended cement-based systems is more evident. For the materials studied in this research, the capillary pores with diameter range of 7.1-73 nm plays dominated role in chloride diffusion under non-saturated state.

Acknowledgements

This research work was carried out in Microlab of Delft University of Technology (*TU Delft*). The authors are grateful for financial support from Chinese Scholarship Council (*CSC*). The cooperation with South China University of Technology (*SCUT*) is highly acknowledged.

References

- ASTM C642-13, 2013. Standard test method for density, absorption and voids in hardened concrete.
- Bertil P., 1997. Moisture in concrete subjected to different kinds of curing. *Materials and Structure*, 30, 533-544
- Badmann R., Stockhausen N., Setzer M. J., 1980. The Statistical Thickness and the Chemical Potential of Adsorbed Water Films. 82 (2), 534-542.
- Chatterji S., 1995. On the applicability of Fick s second law to chloride ion migration through Portland cement concrete. *Cement and Concrete Research*, 25, 299–303.
- Chatterji S., 2004. An explanation for the unsaturated state of water stored concrete. *Cement and Concrete Composites*, 1, 75–79.
- Chen H., Wyrzykowski M., Scrivener K., Lura P., 2013. Prediction of self-desiccation in low water-to-cement ratio pastes based on pore structure evolution. *Cement and Concrete Research*, 49, 38–47.

- Diamond S., 2000. Review-Mercury porosimetry: An inappropriate method for the measurement of pore size distributions in cement-based materials. *Cement and Concrete Research*, 30,1517-1525.
- Galle C., Daian J.F., 2000. Gas permeability of unsaturated cement-based materials: application of a multi-scale network model. *Magazine of Concrete Research*, 52, 251-263.
- Glasser F. P., Zhang L., 2001. High-performance cement matrices based on calcium sulfoaluminate belite composition. *Cement and Concrete Research*, 31, 1881–1886.
- Kaufmann J., Loser R., Leemann A., 2009. Analysis of cement-bonded materials by multi-cycle mercury intrusion and nitrogen sorption. *Journal of Colloid and Interface Science*, 336, 730–737.
- Leonard F. R., 1981. Experimental studies on the applicability of the Kelvin equation to highly curved Concave menisci. *Journal of Colloid and Interface Science*, 80, 528-541.
- Neimark A.V., Ravikovitch P.I., Vishnyakov A., 2003. Bridging scales from molecular simulations to classical thermodynamics: density functional theory of capillary condensation in nanopores. *Journal of Physics: Condensed Matter*, 15 (3), 347-365.
- Nilsson L. O., 1980. Moisture problems at concrete floors. *TVBM-3002. Sweden: Lund Institute of Technology*. 36–51.
- Olsson N., Baroghel-Bouny v., Nilsson L. O., l Thiery M., 2013. Non-saturated ion diffusion in concrete – A new approach to evaluate conductivity measurements. *Cement and Concrete Composites*, 40, 40–47
- Powers T. C., Brownyard T. L., 1947. Studies of the physical properties of hardened Portland cement paste. *Journal American Concrete Institute*, 43-262.
- RILEM TC116-PCD. 1999 'Recommendations: A. Pre-conditioning of concrete test specimens for the measurement of gas permeability and capillary absorption of water'. 32, 174–179.
- Saetta A. V., Scotta R. V. and Vitaliani R. V., 1993. Analysis of Chloride Diffusion into Partially Saturated Concrete. *ACI materials journal*, 19, 441-451.
- Ye G., 2003. Experimental study and numerical simulation of the development of the microstructure and permeability of cementitious materials. *Ph.D. Thesis. Delft.*